CONTRAST INVARIANT AND AFFINE SUB-PIXEL OPTICAL FLOW

Neus Sabater, Sébastien Leprince, and Jean-Philippe Avouac

Geological and Planetary Sciences Division
California Institute of Technology
{sabater, leprincs}@caltech.edu

ABSTRACT

This paper presents the Contrast Invariant and Affine Optical Flow (CIAO), a dense area-based sub-pixel image matching algorithm. CIAO does not force the estimated disparity field between two images to be smooth and allows for contrast and brightness changes. It is robust to drastic changes in the images' content thanks to an adaptive weighting of the neighboring pixels. In addition, the proposed model considers local affine displacements instead of simpler translations. CIAO proves particularly useful to extract high quality, high accuracy, and high density disparity maps from pairs of stereoscopic images. Comparative results with real and synthetic data are provided.

Index Terms— Optical flow, affine and contrast invariant, remote sensing, Digital Elevation Model (DEM), sub-pixel disparity.

1. INTRODUCTION

Although extracting disparity maps from pairs of images has been widely studied, ensuring high accuracy and robustness remains a challenge due to difficult situations arising in natural image sequences. Disparities to be estimated are not usually smooth, contrast variations between images are common, and large occlusions can be present. Dense disparity maps are typically used to recover the 3D information from stereoscopic image pairs, where corresponding points between images must be matched. However, the accuracy of such methods is not usually well documented, and we are here interested in computing disparity maps with sub-pixel accuracy. Image matching methods commonly rely on correlation [1] and phase correlation techniques [2] [3].

The aim of this work is to push further the accuracy limit of image matching techniques by enhancing the well-known optical flow method, which has long been used for 3D reconstruction, and also for motion estimation and image registration problems. Many approaches have been proposed since the publication of the two milestone papers by Horn and Schunck [4] and by Lucas and Kanade [5]. We refer to [6] for a comprehensive review of the different optical flow techniques. The work we present is closer to the approach in [5] since our model does not consider global smoothness constraints as in [4]. In fact, optical flow methods can be separated into locally and globally parameterized methods. The global methods have risen in popularity in the last years [7] because they better solve the aperture problem [8]. Indeed, local image patches may not contain sufficient information to reliably estimate all disparities, causing many outliers in poor textured regions of the images. However, global methods with regularity terms tend to over-smooth the estimated disparity field and are quite sensitive to the parameterization used. For instance, [9] and [10] combine both approaches to strike a balance between local and global methods. Our decision to only focus on local methods stems from two main concerns: (1) Our desire to estimate potentially irregular and discontinuous disparity fields with high accuracy and high spatial resolution; (2) Our desire to propose an algorithm that is adequate for parallel computing with no or little communication between computing cores or nodes, e.g., GPU or distributed computing.

The classic optical flow formulation assumes radiometric consistency between images and a smooth underlying disparity field [7]. However, these assumptions are often too restrictive and make the optical flow technique unsuitable in a general setting, in particular for remote sensing applications. Indeed, such images may have been acquired at different times, under different illuminations, and the disparity field may present variations that are not well approximated by local translations. We introduce the Contrast Invariant and Affine Optical Flow (CIAO), a generalized sub-pixel optical flow model which does not force the estimated disparity field to be smooth, and which allows for contrast and brightness changes by considering bias and gain parameters as suggested in [5]. Furthermore, CIAO is robust to drastic radiometric changes thanks to an adaptive weighting of the neighboring pixels. The algorithm is based on a multi-scale approach since the optical flow linear equation is only a first order approximation. At each scale, when the linear equation is not solvable or when the estimation is unreliable, a bilateral filter [11] extrapolates the disparity field. Finally, the proposed model considers affine displacements instead of simpler translations, which are rarely valid in real scenes with complex disparities. This more complex model produces finer measurements between corresponding points, especially when the images are transformed by a locally large tilt or shear. Indeed, image distortions arising from viewpoint changes are locally well modeled by affine planar transforms. For instance, [12] and [13] already suggested affine models in optical flow for registration and video tracking, respectively. In both cases, an affine deformation is estimated for a large region of the image or for the whole image instead of the local deformations we suggest here. Two relevant formulations appear in [14] and [15] where affine local models in optical flow are considered. In [14] the aim is to compute DEM's from satellite images. The local approach they present is essential for this specific application since a global modeling may not realistically represent the image changes. Their work mainly differs from ours in the parameters estimation (noise and affine parameters) which is performed with a Bayesian approach having high computational complexity. Besides that, the robustness and attainable precision of their method is undocumented. Similar to our approach, [15] also describes a hierarchical approach with an affine model. However, in addition to combining the most audacious ideas found in the literature, we achieve greater accuracy and robustness by introducing

This work was supported by the Keck Institute for Space Studies and by the Gordon and Betty Moore Foundation.

two decisive ideas in optical flow: (i) an accurate interpolation of the images and (ii) a robust method to avoid outliers. To the best of our knowledge such a robustness and accuracy have not been achieved with optical flow techniques making it one of the best methods to compute DEM's for remote sensing applications.

2. THE MATHEMATICAL MODEL

Let $\mathbf{x} = (x, y)$ and $\mathbf{w} = (u, v)$ and let consider the deformation model between two images I_1 and I_2, such that:

$$I_2(\mathbf{x} + \mathbf{w}) = \alpha(\mathbf{x}) \cdot I_1(\mathbf{x}) + \beta(\mathbf{x}) := \tilde{I}_1(\mathbf{x}), \tag{1}$$

where α and β are the parameters controlling the gain and offset at each point, and the local disparity field follows the affine model:

$$\big(u(x,y), v(x,y)\big) = \big(ax + by + c,\ dx + ey + f\big). \tag{2}$$

In order to estimate the disparity $\mathbf{w}$, and inspired by [16], an iterative scheme is proposed, with:

$$\mathbf{w}^0 = (0,0) \quad \text{and} \quad \mathbf{w}^{k+1} = \mathbf{w}^k + \delta\mathbf{w}^k. \tag{3}$$

From now on, we consider the following notations

$$\varphi^k_{\mathbf{x_0}}(\mathbf{x}) := \varphi(\mathbf{x_0}, \mathbf{x}, \mathbf{w}^k), \qquad I^k_x(\mathbf{x}) := \frac{\partial}{\partial x} I_2(\mathbf{x} + \mathbf{w}^k),$$
$$I^k_t(\mathbf{x}) := I_2(\mathbf{x} + \mathbf{w}^k) - \tilde{I}_1(\mathbf{x}), \qquad I^k_y(\mathbf{x}) := \frac{\partial}{\partial y} I_2(\mathbf{x} + \mathbf{w}^k).$$

For each iteration k, the unknown disparity increment $\delta\mathbf{w}^k = (\delta u^k, \delta v^k) = (\delta a^k x + \delta b^k y + \delta c^k, \delta d^k x + \delta e^k y + \delta f^k)$ at $\mathbf{x_0}$ is estimated minimizing:

$$E^{k+1}_{\mathbf{x_0}} = \int_{P_{\mathbf{x_0}}} \varphi^k_{\mathbf{x_0}}(\mathbf{x}) \Big(I_2(\mathbf{x} + \mathbf{w}^{k+1}) - \alpha^k(\mathbf{x_0}) \cdot I_1(\mathbf{x}) - \beta^k(\mathbf{x_0}) \Big)^2 d\mathbf{x}, \tag{4}$$

where $P_{\mathbf{x_0}}$ is an image patch centered at $\mathbf{x_0}$ and φ is an adaptive function weighting the quadratic error such that:

$$\varphi^k_{\mathbf{x_0}}(\mathbf{x}) = \exp\Big(\frac{-||\mathbf{x_0} - \mathbf{x}||^2}{2\sigma_1^2}\Big) \cdot \exp\Big(\frac{-I^k_t(\mathbf{x})^2}{2\sigma_2^2}\Big) \cdot \chi_{[|I^k_t(\mathbf{x})| < 2\sigma_2]}, \tag{5}$$

where χ is the characteristic function. Note that the first exponential term is a spatial weighting and the second term penalizes the pixels in the patch where $I_2(\mathbf{x} + \mathbf{w}^k)$ differs considerably from $\tilde{I}_1(\mathbf{x})$ at iteration k. When this difference is too large, the third term is null. Therefore, if an object in the scene appears differently between the two images, the pixels of that object are considered with smaller weights than the more similar pixels, or they are simply disregarded if the difference is too large (e.g., occlusions).

In practice, the contrast change parameters α and β are computed before the energy minimization using:

$$\beta^k(\mathbf{x_0}) = \overline{I_2(\mathbf{x_0} + \mathbf{w}^k)} - \overline{I_1(\mathbf{x_0})}, \tag{6}$$

$$\alpha^k(\mathbf{x_0}) = \frac{\int_{P_{\mathbf{x_0}}} \varphi^k_{\mathbf{x_0}} \big(I_2(\mathbf{x} + \mathbf{w}^k) - \beta^k(\mathbf{x_0})\big) I_1(\mathbf{x})\, d\mathbf{x}}{\int_{P_{\mathbf{x_0}}} \varphi^k_{\mathbf{x_0}} I_1^2(\mathbf{x})\, d\mathbf{x}}, \tag{7}$$

where $\overline{I(\mathbf{x})}$ indicates the gray mean value of I over $P_{\mathbf{x}}$. Remark that this choice of parameters allows local affine contrast changes. In particular, β subtracts the gray mean value of the image patches in Eq. (4) compensating the image offset and α is the bias parameter such that:

$$\alpha^k(\mathbf{x_0}) = \arg\min_{\lambda} \int_{P_{\mathbf{x_0}}} \varphi^k_{\mathbf{x_0}}(\mathbf{x}) \Big(I_2(\mathbf{x} + \mathbf{w}^k) - \lambda\, I_1(\mathbf{x}) - \beta^k(\mathbf{x_0}) \Big)^2 d\mathbf{x}. \tag{8}$$

Then, the minimum of $E^{k+1}_{\mathbf{x_0}}$ is reached when the partial derivatives are zero, i.e.:

$$\frac{\partial}{\partial\, \delta a^k} E^{k+1}_{\mathbf{x_0}} = 0 \Leftrightarrow \int x\, \varphi^k_{\mathbf{x_0}}\, I^{k+1}_t\, I^{k+1}_x d\mathbf{x} = 0, \tag{9}$$

and similarly for the derivatives w.r.t. $\delta b^k, \delta c^k, \delta d^k, \delta e^k$ and δf^k.

Now, using Eq. (3) we write the first order Taylor expansions:

$$I^{k+1}_t = I^k_t + I^k_x\, \delta u^k + I^k_y\, \delta v^k, \tag{10}$$

$$I^{k+1}_x = I^k_x + I^k_{xx}\, \delta u^k + I^k_{xy}\, \delta v^k, \tag{11}$$

$$I^{k+1}_y = I^k_y + I^k_{xy}\, \delta u^k + I^k_{yy}\, \delta v^k. \tag{12}$$

Since the disparity increments are supposed to be small, the terms containing $(\delta u^k)^2$, $(\delta v^k)^2$, and $(\delta u^k \cdot \delta v^k)$ can be neglected and from Eq. (9) we obtain the linear system:

$$\mathbf{A}^k\, \mathbf{X}^k = \mathbf{B}^k, \tag{13}$$

where $\mathbf{X}^k = (\delta a^k \quad \delta b^k \quad \delta c^k \quad \delta d^k \quad \delta e^k \quad \delta f^k)^T$ (see the next top page for $\mathbf{A}^k$ and $\mathbf{B}^k$.)

When the displacement to be estimated is greater than one pixel, Eq. (13) will unlikely hold. Nevertheless, large disparities can be estimated with a multi-scale approach, where the result of the last iteration at a coarse scale is used as initialization in a finer scale.

2.1. Detecting and removing outliers

To decrease the number of outliers, [17] introduced robust cost functions instead of the least-squares estimation, and [8] suggested to jointly estimate the outlier process and the disparities with a probabilistic mixture framework. However, these techniques do not completely rule out outliers in real scenes with complex situations (poor textured regions, moving or disappearing objects, non local radiometry changes, etc.) In these situations, an incorrect disparity can be estimated at a certain scale, and propagated to the next ones. In our model, the second and third penalty terms in the weighting function (Eq. (5)) meaningfully attenuate that problem. CIAO also considers two extra security tests which, combined with the weighting function, are able to discard most false matches. More precisely, we will consider that $\delta\mathbf{w}^k(\mathbf{x}) = \emptyset$ when

- The linear system is not solvable: $\text{rcond}(\mathbf{A}^k) < 0.001$[1], where $\mathbf{A}^k$ is the associated matrix computed over $P_{\mathbf{x}}$.
- The displacement is not consistent with the mathematical model: $\delta\mathbf{w}^k(\mathbf{x}) > 1$ pixel.

Then, an iterative bilateral filter extrapolates the empty disparity values.

3. THE CIAO ALGORITHM

At each scale, 3 iterations are performed. At each iteration k the following steps are performed:

1. Compute I^k_t by warping the second image I_2
2. Compute $\varphi(\mathbf{x_0}, \mathbf{x}, \mathbf{w}^k)$, $\forall \mathbf{x_0}$ using Eq. (5) ($\alpha = 1$, $\beta = 0$)
3. Compute $\alpha^k(\mathbf{x_0})$, $\beta^k(\mathbf{x_0})$, $\forall \mathbf{x_0}$ using Eq. (6) and Eq. (7)
4. Update $\varphi(\mathbf{x_0}, \mathbf{x}, \mathbf{w}^k)$

[1] rcond($\mathbf{A}$) is an estimate of the reciprocal of the condition of $\mathbf{A}$

$$\mathbf{A^k} = \begin{pmatrix} \int x^2\,\varphi^k_{\mathbf{x_0}}(I^k_x)^2 & \int x\,y\,\varphi^k_{\mathbf{x_0}}(I^k_x)^2 & \int x\,\varphi^k_{\mathbf{x_0}}(I^k_x)^2 & \int x^2\,\varphi^k_{\mathbf{x_0}} I^k_x\,I^k_y & \int x\,y\,\varphi^k_{\mathbf{x_0}} I^k_x\,I^k_y & \int x\,\varphi^k_{\mathbf{x_0}} I^k_x\,I^k_y \\ \int x\,y\,\varphi^k_{\mathbf{x_0}}(I^k_x)^2 & \int y^2\,\varphi^k_{\mathbf{x_0}}(I^k_x)^2 & \int y\,\varphi^k_{\mathbf{x_0}}(I^k_x)^2 & \int x\,y\,\varphi^k_{\mathbf{x_0}} I^k_x\,I^k_y & \int y^2\,\varphi^k_{\mathbf{x_0}} I^k_x\,I^k_y & \int y\,\varphi^k_{\mathbf{x_0}} I^k_x\,I^k_y \\ \int x\,\varphi^k_{\mathbf{x_0}}(I^k_x)^2 & \int y\,\varphi^k_{\mathbf{x_0}}(I^k_x)^2 & \int \varphi^k_{\mathbf{x_0}}(I^k_x)^2 & \int x\,\varphi^k_{\mathbf{x_0}} I^k_x\,I^k_y & \int y\,\varphi^k_{\mathbf{x_0}} I^k_x\,I^k_y & \int \varphi^k_{\mathbf{x_0}} I^k_x\,I^k_y \\ \int x^2\,\varphi^k_{\mathbf{x_0}} I^k_x\,I^k_y & \int x\,y\,\varphi^k_{\mathbf{x_0}} I^k_x\,I^k_y & \int x\,\varphi^k_{\mathbf{x_0}} I^k_x\,I^k_y & \int x^2\,\varphi^k_{\mathbf{x_0}}(I^k_y)^2 & \int x\,y\,\varphi^k_{\mathbf{x_0}}(I^k_y)^2 & \int x\,\varphi^k_{\mathbf{x_0}}(I^k_y)^2 \\ \int x\,y\,\varphi^k_{\mathbf{x_0}} I^k_x\,I^k_y & \int y^2\,\varphi^k_{\mathbf{x_0}} I^k_x\,I^k_y & \int y\,\varphi^k_{\mathbf{x_0}} I^k_x\,I^k_y & \int x\,y\,\varphi^k_{\mathbf{x_0}}(I^k_y)^2 & \int y^2\,\varphi^k_{\mathbf{x_0}}(I^k_y)^2 & \int y\,\varphi^k_{\mathbf{x_0}}(I^k_y)^2 \\ \int x\,\varphi^k_{\mathbf{x_0}} I^k_x\,I^k_y & \int y\,\varphi^k_{\mathbf{x_0}} I^k_x\,I^k_y & \int \varphi^k_{\mathbf{x_0}} I^k_x\,I^k_y & \int x\,\varphi^k_{\mathbf{x_0}}(I^k_y)^2 & \int y\,\varphi^k_{\mathbf{x_0}}(I^k_y)^2 & \int \varphi^k_{\mathbf{x_0}}(I^k_y)^2 \end{pmatrix} \tag{14}$$

$$\mathbf{B^k} = \Big(\int x\,\varphi^k_{\mathbf{x_0}} I^k_t\,I^k_x \quad \int y\,\varphi^k_{\mathbf{x_0}} I^k_t\,I^k_x \quad \int \varphi^k_{\mathbf{x_0}} I^k_t\,I^k_x \quad \int x\,\varphi^k_{\mathbf{x_0}} I^k_t\,I^k_y \quad \int y\,\varphi^k_{\mathbf{x_0}} I^k_t\,I^k_y \quad \int \varphi^k_{\mathbf{x_0}} I^k_t\,I^k_y \Big)^T \tag{15}$$

5. Estimate the disparity increment $\delta\mathbf{w}^k$ using Eq. (13)
6. Extrapolate the disparity field using the bilateral filter [11] for the points where no displacement has been found.
7. $\mathbf{w}^{k+1} = \mathbf{w}^k + \delta\mathbf{w}^k$

The parameters of the algorithm have been fixed once to the values: size of the patch image $P_\mathbf{x} = s \times s$ with $s = 11$ pixels, $\sigma_1 = s/3$ pixels and $\sigma_2 = 5$.

To increase computational speed, the disparity model at the coarsest scales is only a translation model, the affine model being only necessary at the last and finest scale.

Second image warping The first step of the algorithm at each iteration performs a warping of the second image using the estimated displacement from the previous iteration. Traditionally, this is accomplished using a bicubic [7] (or bilinear [14]) interpolation method, but we have seen that this entails a significant loss of accuracy. Instead, we propose to use a sinc interpolation. Indeed, we have used a truncated sinc (with size 17×17) in the last scale which is a reasonable increase of complexity while the accuracy improves by a factor of 10 (see Fig. 1-c). The remaining error still has a periodic pattern, which could be further reduced using a larger kernel but at a larger computational cost. The parameters used provide a good compromise between accuracy and complexity.

4. EXPERIMENTAL RESULTS

To illustrate the difference between the translation and the affine model, we have performed a test where the second image has been simulated from the first image (Fig. 1-a) with an affine horizontal displacement (Fig. 1-b). Fig. 1-d shows the difference between the same algorithm using the affine model at the finest scale, or only using the translative model. In this error profile we observe that the result is noisier when only the translative model is considered. The periodic pattern of the error, which has a maximal amplitude of $3/1000$ pix., comes from the limited support of the sinc interpolator used to warp the image.

To quantify the error close to disparity discontinuities we have simulated, using the same image as in Fig. 1-a, a piecewise affine displacement in the horizontal direction (see the profile of the displacement in Fig 2-a). We observe in Fig. 2-b that the error profile around the discontinuity is considerably larger ($\approx$1 pix) with the translative model than with the affine model ($\approx$0.4 pix). The larger error appears in a region of 11 pixel wide, which is the size of our window patch $P_\mathbf{x}$. Smaller windows will decrease the errors at the discontinuities but the overall result will be noisier.

Fig. 3 compares the result of the CIAO algorithm on real satellite (SPOT) images with the state-of-the-art algorithm presented in [7]. Images were acquired before and after the 1999 Mw 7.1 Hector Mine earthquake with two years interval [2], showing shadowing and texture differences. In this example, the North-South fault displacement appears clearly in our sub-pixel disparity field, where the maximum disparity offset is on the order of 1/2 of the pixel size. On the contrary, the algorithm presented in [7] is completely false because of the outliers and the over-smoothing of the regularity term. Finally, the results obtained with two other algorithms published on line in [18] and [19] can be seen in the public archives of their website[2].

5. CONCLUSION

We presented CIAO, a new optical flow algorithm to estimate locally affine disparity maps with sub-pixel accuracy. On the one hand, our results show that the affine model is more accurate than the classic translative model over smooth surfaces and around discontinuities. Indeed, the disparity error of our algorithm is smaller than $3/1000$ of the pixel size for smooth disparities, and it is 60% smaller than that obtained from a translative model around disparity discontinuities. On the other hand, we have shown that the sinc interpolation used in our algorithm improves the accuracy by a factor of 10 compared to bicubic interpolation.To the best of our knowledge, the sub-pixel accuracy reached by CIAO has not been rivaled by any other optical flow method (the website http://vision.middlebury.edu/flow evaluates different optical flow methods but the groundtruth is not accurate enough to validate very precise sub-pixel algorithms [1]). Furthermore, CIAO is robust to significant changes in the image content thanks to its mathematical model, which allows for contrast changes and includes an adaptive weighting function. Further research will be directed to automatically adapt the parameter σ_2 depending on the local image dynamic. Accurately and robustly estimating disparity maps is a crucial element to derive high quality digital elevation models from aerial or satellite stereoscopic images. In fact, CIAO will be used to process a great amount of satellite images to measure very precisely ground deformations, which is of uttermost interest to Earth Sciences.

6. REFERENCES

[1] N. Sabater, J.M. Morel, and A. Almansa, "How accurate can block matches be in stereovision?," *SIAM Journal on Imag. Sciences*, vol. 4, pp. 472–500, 2011.

[2] S. Leprince, S. Barbot, F. Ayoub, and J. P. Avouac, "Automatic and precise ortho-rectification, coregistration, and subpixel correlation of satellite images, application to ground deformation measurements.," *TGARS*, vol. 45, pp. 6, 2007.

[3] D. Scharstein and R. Szeliski, "A taxonomy and evaluation of dense two-frame stereo correspondence algorithms," *IJCV*, vol. 47, pp. 7–42, 2002.

[2] http://www.ipol.im/pub/demo/sm_horn_schunck/archive and http://www.ipol.im/pub/demo/smf_tvl1_optical_flow_estimation/archive

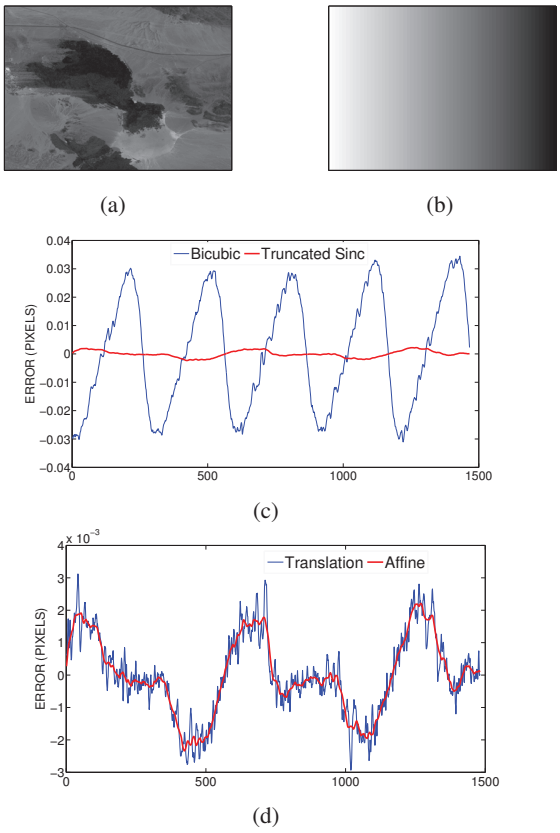

Fig. 1. (a) Original Image. (b) Disparity ground truth with values in [0,5] pix. The second image has been simulated by warping the original image with this displacement. (c) Disparity error profile using only bicubic interpolation (blue) or using a truncated sinc at the last scale (red). (d) Error profile with sinc warping using an affine model (red) and a translative model (blue).

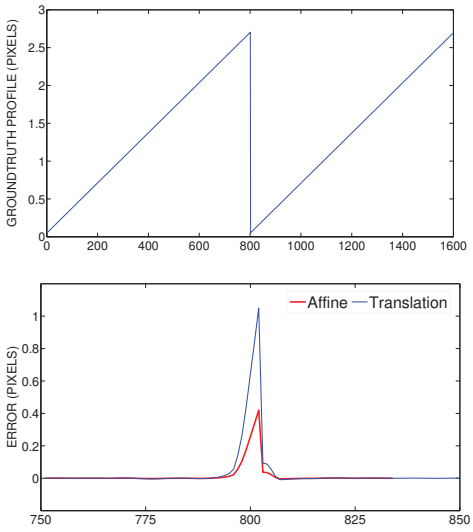

Fig. 2. Synthetic data simulating a disparity discontinuity. Top: disparity groundtruth profile. Bottom: disparity error plot around the discontinuity with a translative model (blue) and an affine model (red).

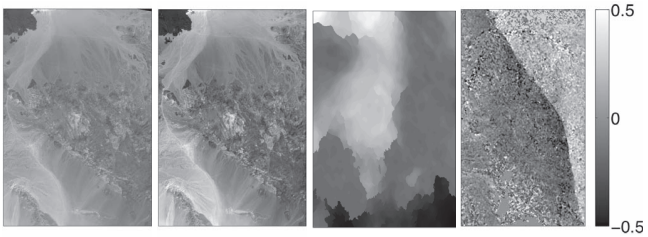

Fig. 3. From left to right: first and second images, result obtained with [7] and the sub-pixel disparity field obtained with CIAO along image columns (North-South). The local and sub-pixel algorithm we propose corresponds to the real fault displacement (see [2]) and is more robust and accurate than [7] (one of the state-of-the-art algorithms) in complicated scenes as this one.

[4] B. K. P. Horn and B. G. Schunck, "Determining optical flow," *Artificial Intelligence*, vol. 17, pp. 185–203, 1981.

[5] B. D. Lucas and T. Kanade, "An iterative image registration technique with an application to stereo vision," in *IJCAI*, 1981.

[6] J. L. Barron, D. J. Fleet, and S. S. Beauchemin, "Performance of optical flow techniques," *IJCV*, vol. 12, pp. 43–77, 1994.

[7] D. Sun, S Roth, and J.M. Black, "Secrets of optical flow estimation and their principles," in *CVPR*, 2010.

[8] A. Jepson and Black J.M., "Mixture models for optical flow computation," in *CVPR*, 1993.

[9] A. Bruhn, J. Weickert, and C. Schnörr, "Lucas/kanade meets horn/schunck: combining local and global optic flow methods," *IJCV*, vol. 61, pp. 211–231, 2005.

[10] S.X. Ju, M.J. Black, and A.D. Jepson, "Skin and bones: Multilayer, locally affine, optical flow and regularization with transparency," *CVPR*, 1996.

[11] C. Tomasi and R. Manduchi, "Bilateral filtering for gray and color images," in *ICCV*, 1998.

[12] Y. Altunbasak, R.M. Mersereau, and A.J. Patti, "A fast parametric motion estimation algorithm with illumination and lens distortion correction," *TIP*, vol. 12, pp. 395 – 408, 2003.

[13] F. G. Meyer and P. Bouthemy, "Region-based tracking using affine motion models in long image sequences," *CVGIP: Image Underst.*, vol. 60, pp. 119–140, 1994.

[14] M.J. Broxton, A.V. Nefian, Z. Moratto, T. Kim, M. Lundy, and A.V. Segal, "3d lunar terrain reconstruction from apollo images," in *Int. Symp. on Advances in Visual Computing*, 2009.

[15] J.-Y. Bouguet, "Pyramidal implementation of the affine lucas kanade feature tracker. description of the algorithm," Tech. Rep., Microsoft, 2001.

[16] T. Brox, A. Bruhn, N. Papenberg, and J. Weickert, "High accuracy optical flow estimation based on a theory for warping," in *ECCV*, 2004.

[17] M.J. Black and P. Anandan, "The robust estimation of multiple motions: parametric and piecewise-smooth flow fields," *CVIU*, vol. 63, pp. 75–104, 1996.

[18] *www.ipol.im/pub/algo/sm_horn_schunck*, 2011.

[19] *www.ipol.im/pub/algo/smf_tvl1_optical_flow_estimation*, 2011.